Solutions of Poisson Equation Within Singly and Doubly Connected Prismatic Domains

M.M. Yovanovich* and Y.S. Muzychka†

Department of Mechanical Engineering
University of Waterloo
Waterloo, Ontario, Canada N2L 3G1

Solutions to Poisson's equation in singly and doubly-connected domains are examined. Applications for steady heat conduction with uniformly distributed heat sources and fully developed viscous fluid flow are discussed. By means of dimensional analysis the appropriate characteristic length and non-dimensional groups are proposed for presenting the results of many geometries. It is shown that the dimensionless groups based upon the square root of the cross-sectional area are weak functions of the shape of the geometry provided an appropriate aspect ratio is defined. Finally, it is shown that the solution for the elliptic geometry and circular annular geometry may be used to accurately compute results for 27 singly-connected domains and 9 doubly-connected domains, respectively.

NOMENCLATURE

A	=	flow area, m^2
a	=	major axis of ellipse or rectangle, m
b	=	minor axis of ellipse of rectangle, m
c	=	radial and/or linear dimension, see Fig. 2, m
$\mathcal{B}$	=	boundary of a domain
D	=	diameter of circular duct, m
D_h	=	hydraulic diameter, $\equiv 4A/P$
$E(\cdot)$	=	complete elliptic integral second kind
f	=	friction factor $\equiv \overline{\tau}/(\frac{1}{2}\rho\overline{w}^2)$
$g(\epsilon)$	=	shape function
k	=	thermal conductivity, W/mK
L	=	length of domain, m
N	=	number of sides of polygons
n	=	hyperellipse shape parameter
P	=	perimeter, m
p	=	pressure, N/m^2
$Po_{\mathcal{L}}$	=	Poiseuille number, $\equiv \overline{\tau}_w\mathcal{L}/\mu\overline{w}$
q	=	heat flux, W/m^2
r	=	radius of circular duct, m
r^*	=	dimensionless radius ratio, $\equiv r_i/r_o$
$Re_{\mathcal{L}}$	=	Reynolds number, $\equiv \overline{w}\mathcal{L}/\nu$
$\mathcal{S}$	=	volumetric heat source, W/m^3
T	=	temperature, K
w	=	axial velocity, m/s

Greek Symbols

β	=	aspect ratio, $\equiv \sqrt{A_i/A_o}$
ϵ	=	aspect ratio, $\equiv b/a$
ϕ	=	dimensionless velocity or temperature
Φ	=	angular measurement, see Fig. 2
θ	=	temperature excess, $T - T_b$, K
μ	=	dynamic viscosity, Ns/m^2
ν	=	kinematic viscosity, m^2/s
ρ	=	fluid density, kg/m^3
τ	=	wall shear stress, N/m^2

Subscripts

$\sqrt{A}$	=	based upon square root of area
b	=	boundary
c	=	circumscribed
D_h	=	based upon hydraulic diameter
$\mathcal{L}$	=	based upon arbitrary length $\mathcal{L}$
H	=	hydrodynamic
i	=	inner, inscribed
o	=	outer
T	=	thermal
w	=	wall

Superscripts

$\overline{(\cdot)}$	=	denotes average value of $(\cdot)$
C	=	circular
E	=	elliptical
P	=	polygonal
R	=	rectangular

INTRODUCTION

Steady conduction within long singly- and doubly-connected prismatic rods of constant thermal conductivity and constant arbitrary cross-section in which there are uniformly distributed heat sources is of some interest to thermal analysts. The relationship between the area-mean temperature and the average boundary heat flux when the

*Professor, Fellow AIAA

†Graduate Research Assistant

boundary temperature is taken to be constant is required.

The current undergraduate heat transfer texts, graduate conduction texts and the heat transfer handbook deal with a small number of examples such as the circular singly and doubly-connected rods, the singly-connected rectangular and square rods, and the elliptical rod. Solutions for other important shapes are presently unavailable.

There are four objectives for this work. One objective is to report results which are available in the open literature. A second objective is to present solutions for several shapes such as singly-connected regular polygons which include the equilateral triangle, the square, pentagon, etc., rectangular, elliptical, triangular and other miscellaneous geometries (see Figs. 1 and 2). Doubly-connected rods which are either (i) bounded internally by regular polygons and bounded externally by a circle, (ii) bounded internally by a circle and bounded externally by regular polygons, and (iii) bounded internally and externally by similar polygons, (see Fig. 3). In all cases as the number of sides of the polygon increases, the cross-sections approach the circular annulus.

A third objective is to introduce a non-dimensional parameter which is based on the cross-section shape parameters such as the total perimeter and the cross-sectional area, the thermal conductivity, the source strength and the mean temperature of the cross-section. It will be shown by means of dimensional analysis that the proposed dimensionless group is a weak function of the shape of the cross-section provided the appropriate characteristic length is chosen.

A fourth objective is to show that the conduction problem is related to the problem of fully-developed laminar flow through ducts of different cross-sections. It will be shown that the analogy between the two quite different physical problems is strong and therefore the many results available in the fluids texts such as White[1], Happel and Brenner[2], Shah and London[3] can be applied to the analogous conduction problem.

MATHEMATICAL FORMULATION

The thermal and hydrodynamic problems will be stated first in dimensional form, followed by the non-dimensional formulation to illustrate the similarity of the two problems.

Dimensional Thermal Problem

The governing differential equation and boundary conditions for the thermal problem are:

$$\frac{\partial^2 T}{\partial x^2} + \frac{\partial^2 T}{\partial y^2} = -\frac{\mathcal{S}}{k} \tag{1}$$

where $T(x, y)$ is the temperature within the singly- or doubly-connected domain. The thermal parameters are the constant and uniform volumetric source strength $\mathcal{S}$ and the thermal conductivity k. The boundary conditions are (i) $T = T_b$ at all points on the inner and outer boundaries $\mathcal{B}_i$ and $\mathcal{B}_o$ respectively of the doubly-connected domain, and (ii) $T(x, y) \neq \infty$ within the domain. Introduction of the temperature excess $\theta = T(x, y) - T_b$ leads to the homogeneous boundary condition of the first kind, $\theta = 0$, at all points on the inner and outer boundaries $\mathcal{B}_i$ and $\mathcal{B}_o$.

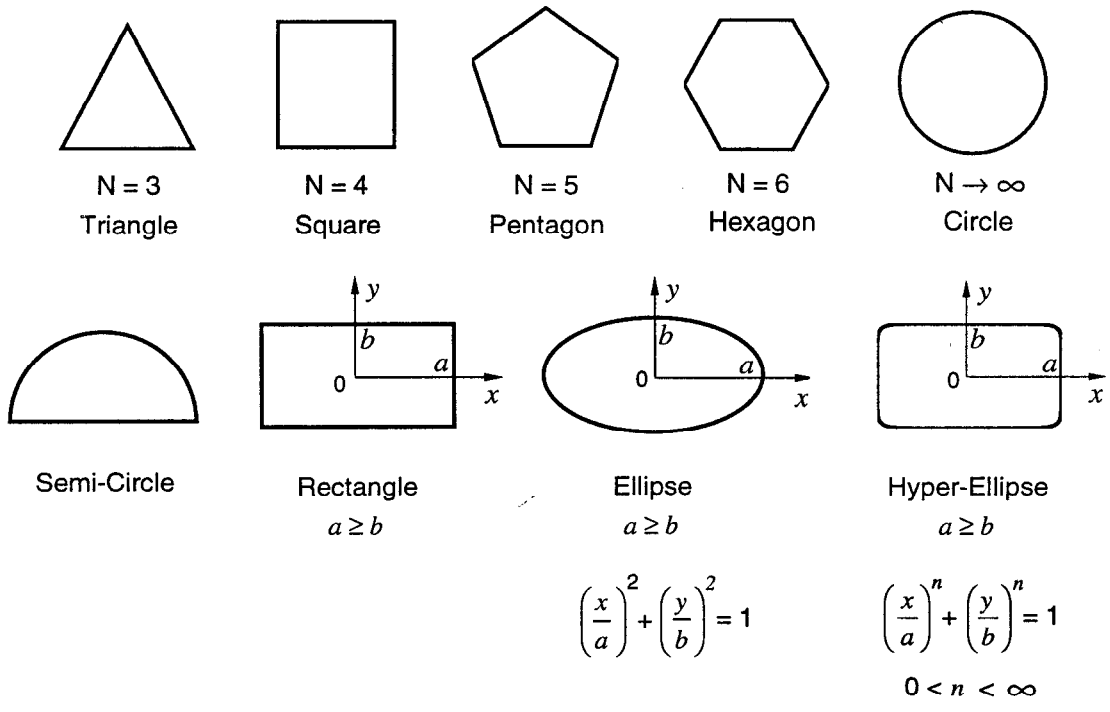

Fig. 1 Common singly-connected geometries

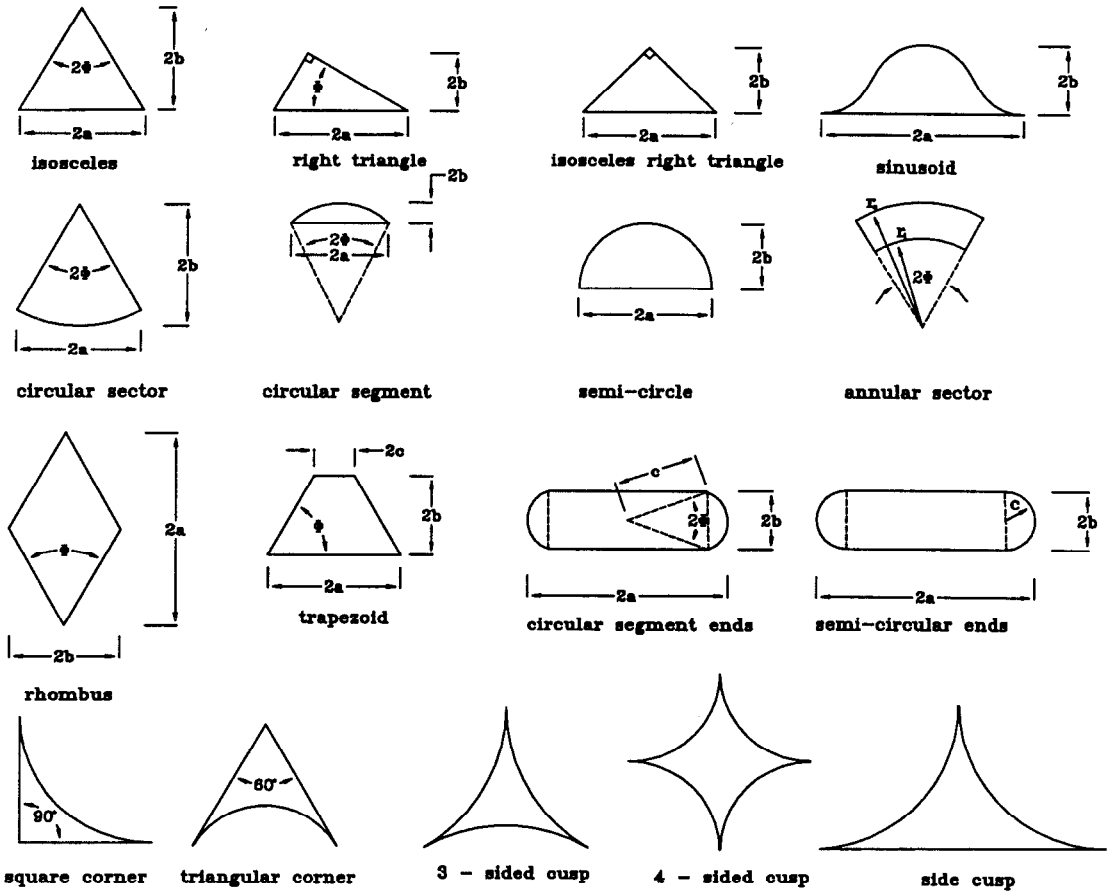

Fig. 2 Other singly-connected geometries

Dimensional Hydrodynamic Problem

The corresponding hydrodynamic problem for steady fully-developed laminar flow of a viscous fluid through a doubly-connected duct or pipe is

$$\frac{\partial^2 w}{\partial x^2} + \frac{\partial^2 w}{\partial y^2} = -\frac{1}{\mu}\frac{\Delta p}{L} \tag{2}$$

where $w(x,y)$ is the axial velocity, μ is the viscosity, $\Delta p = p_1 - p_2$ is the pressure drop over the duct length L. The no-slip condition requires the homogeneous boundary condition $w(x,y) = 0$ at all points of the inner and outer boundaries. The boundedness condition requires that $w(x,y) \neq \infty$ within the cross-section.

Non-dimensional Thermal and Hydrodyanamic Problem

The thermal and hydrodynamic problems given above can be transformed into the same non-dimensional problem by the introduction of the non-dimensional temperature and velocity. The non-dimensional temperature ϕ_T and non-dimensional velocity ϕ_H are defined as

$$\phi_T = \frac{k\theta}{\mathcal{L}^2 \mathcal{S}} \tag{3}$$

and

$$\phi_H = \frac{\mu w}{\mathcal{L}^2 \Delta p / L} \tag{4}$$

where $\mathcal{L}$ is some scale length of the cross-section. In fluid mechanics the scale length is frequently taken to be the hydraulic diameter defined as

$$\mathcal{L} = D_h = \frac{4A}{P} \tag{5}$$

where $A = A_o - A_i$ is the flow area and P is the total wetted perimeter. It will be shown in subsequent sections that there is another more appropriate scale length for both problems.

For all subsequent discussions the non-dimensional temperature and velocity will be denoted as ϕ without the subscripts.

The non-dimensional Poisson differential equation becomes

$$\frac{\partial^2 \phi}{\partial \eta^2} + \frac{\partial^2 \phi}{\partial \zeta^2} = -1 \tag{6}$$

where $\eta = x/\mathcal{L}$ and $\zeta = y/\mathcal{L}$ are the dimensionless cartesian coordinates. The non-dimensional boundary conditions become (i) $\phi = 0$ at all points on the inner and outer boundaries of the cross-section, and (ii) $\phi \neq \infty$ for all points within the cross-section. The two-dimensional Poisson equation given above applies to other physical problems

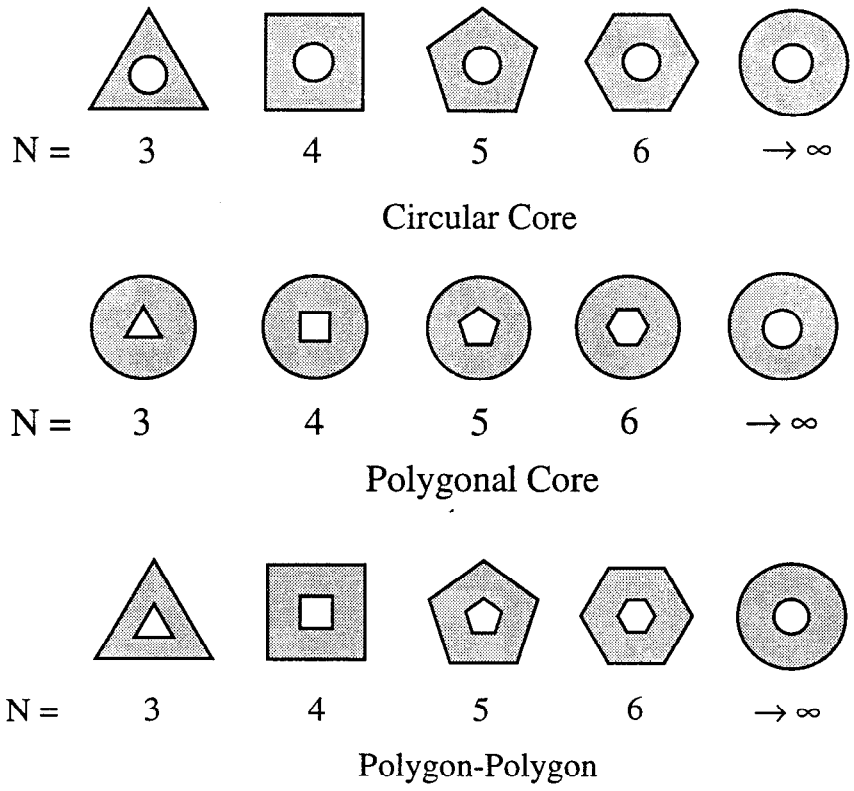

Fig. 3 Various doubly-connected geometries

such as the torsion of a long prismatic rod, the displacement of a thin membrane stretched over the cross-section, and the rotation of an inviscid fluid in a long container of constant cross-section. Several analytical and numerical methods have been employed to find solutions for different geometries.

One objective of this work is to obtain a relationship for the area-mean temperature and area-mean velocity and the geometric and physical parameters of the cross-section. The area-mean dimensionless temperature or velocity is defined as

$$\overline{\phi} = \frac{1}{A}\int\int_A \phi \, dA \tag{7}$$

The dimensionless area-mean velocity is related to the Poiseuille number $1/Po = \mu\overline{w}/(\Delta P/L)\mathcal{L}^2$, Churchill[4].

Dimensionless Thermal and Hydrodynamic Groups

A thermal energy balance over a macro-control volume leads to the dimensionless group which brings the mean wall heat flux and the mean cross-section temperature together:

$$N_T = \frac{\overline{q}_w \mathcal{L}}{k\overline{\theta}} \tag{8}$$

A force balance over a macro-control volume leads to the dimensionless group which brings together the mean wall shear and the mean cross-section velocity together:

$$N_H = \frac{\overline{\tau}_w \mathcal{L}}{\mu\overline{w}} \tag{9}$$

In fluid mechanics there is a tradition of introducing the friction factor f into the dimensionless group N_H. The friction factor is defined as[1,3,4]

$$f = \frac{\overline{\tau}_w}{\frac{1}{2}\rho\overline{w}^2} \tag{10}$$

The hydrodynamic group with the introduction of the Reynolds number

$$Re_{\mathcal{L}} = \frac{\rho\overline{w}\mathcal{L}}{\mu} \tag{11}$$

becomes

$$N_H = \frac{1}{2} f Re_{\mathcal{L}} \tag{12}$$

Since the thermal and hydrodynamic groups are mathematically identical, one can write the following relation between the thermal and hydrodynamic groups:

$$\frac{\overline{q}_w \mathcal{L}}{k\,\overline{\theta}} = \frac{1}{2} f Re_{\mathcal{L}} \tag{13}$$

The energy balance on a macro-control volume gives the relation for the mean wall heat flux:

$$\bar{q}_w = \mathcal{S}\frac{A}{P} \tag{14}$$

which gives the desired relation between the thermal and the hydrodynamic problems:

$$\frac{\mathcal{S}A\mathcal{L}}{k\,\bar{\theta}P} = \frac{1}{2} f Re_{\mathcal{L}} \tag{15}$$

The unknown area-mean temperature excess appears in the denominator and all of the other geometric and thermal parameters are known. The convention in fluid mechanics is to select the hydraulic diameter as the length scale. Introduction of this length scale into the previous relation gives:

$$\frac{\mathcal{S}A\mathcal{L}}{k\,\bar{\theta}P} = \frac{1}{8}\frac{\mathcal{L}P}{A} f Re_{D_h} \tag{16}$$

In the subsequent sections dimensional analysis will be employed to select the appropriate scale length for singly-connected cross-sections such as those shown in Fig. 1 and 2. Once the appropriate scale length has been selected, it will be shown that the dimensionless groups are weak functions of the shape of the cross-section when an appropriate aspect ratio is defined.

DIMENSIONAL ANALYSIS

Dimensional analysis using the Buckingham Π theorem has been applied to many physical phenomena such as fluid flow, heat transfer, stress and strain, and electromagnetic field theory[5-7]. The basic theory of dimensional analysis is still presented in most elementary fluid mechanics texts[8,9], however, its inclusion in heat transfer texts is non-existent, except for the early texts by McAdams[10] and Rohsenow and Choi[11]. Dimensional analysis using the Buckingham Π theorem is one of many methods for determining the important non-dimensional groups in problems which contain many dimensional parameters.

In many of the classic texts on dimensional analysis[5-7], examples are given only for simple geometries such as the circular duct or circular cylinder. Application to non-circular geometries pre-supposes the use of concepts such as the hydraulic diameter or other equivalent length scales. In the next section, application of the Buckingham Π theorem to the two problems discussed earlier will be conducted from a general perspective. The results of this analysis will be applied to several different geometries and a simple model which is valid for all of the geometries discussed will be developed.

Thermal Problem

The variables of interest for the thermal problem are listed below.

$$f(\bar{\theta}, \mathcal{S}, k, A, P) = 0 \tag{17}$$

In order to apply the Π theorem, the number of Π groups must be determined. The Π theorem states that if there are m variables and r fundamental units, then there will be $(m-r)$ Π groups. However, this classical approach does not always yield a solution. In such cases, the value of r is then decreased by one and the method repeated. This approach is generally presented in more elementary texts such as Vennard and Street[8] and White[9]. A more formal approach is presented in the advanced text by Panton[12] or the texts on dimensional analysis by Huntly[5], Langhaar[6] and Taylor[7]. The number of Π groups is determined by examining the dimensional matrix and determining its rank. The rank of the dimensional matrix is the order of the largest square sub-matrix which has a non-zero determinant. The dimensional matrix is given below for the mass (M), length (L), time (T) and temperature (Θ) system of units.

	$\mathcal{S}$	$\bar{\theta}$	A	P	k
M	1	0	0	0	1
L	-1	0	2	1	1
T	-3	0	0	0	-3
Θ	0	1	0	0	-1

Examination of the dimensional matrix reveals that no 4×4 matrix has a non-zero determinant. A 3×3 nonzero determinant may be found. The repeating variables for the Π theorem analysis are chosen to be those that form any 3×3 matrix with a non-zero determinant. Several combinations are possible. The repeating variables will be chosen to be $\bar{\theta}$, k and A. Another possible combination is $\bar{\theta}$, $\mathcal{S}$, and A. These two combinations produce identical Π groups. If the perimeter of the duct P is exchanged for the cross-sectional area A, then another set of Π groups will be formed from the new set of repeating variables. In all cases there is one common Π group. Combinations of variables with area A are more favorable since the product $\mathcal{S}A$ which appears has more physical meaning than the product $\mathcal{S}P^2$.

Having determined the rank of the matrix to be three, there will be two Π groups. Therefore the problem may be more compactly stated in the following dimensionless form of Eq. (17):

$$\phi(\pi_1, \pi_2) = 0 \tag{18}$$

Proceeding with the analysis as outlined in any of the references[5-9,12], the resulting Π groups are found to be

$$\pi_1 = \frac{\mathcal{S}A}{\bar{\theta}k}, \quad \pi_2 = \frac{P}{\sqrt{A}} \tag{19}$$

Now in this case, since there are only two Π groups, Eq. (18) may be written in the following form:

$$\frac{\mathcal{S}A}{\bar{\theta}k} = C\frac{P}{\sqrt{A}} \tag{20}$$

or it may be expressed as

$$\frac{\mathcal{S}A}{\bar{\theta}k}\frac{\sqrt{A}}{P} = C \tag{21}$$

where C is a constant. Finally, by performing a control volume heat balance at the surface of the solid one arrives at the following relation for the surface heat flux:

$$\mathcal{S}A = \overline{q}_w P \tag{22}$$

This leads to the final form of the dimensionless wall flux:

$$\frac{\overline{q}_w \sqrt{A}}{\overline{\theta} k} = C \tag{23}$$

Hydrodynamic Problem

In the case of the analogous hydrodynamic problem the important variables are

$$f(\overline{w}, -\frac{dp}{dz}, \mu, A, P) = 0 \tag{24}$$

In many of the classic texts[5-9], the density of the fluid is also included in the Π analysis. Use of the fluid density is not required since the fully developed duct flow problem represents a balance of pressure and viscous forces. If density is included, then an additional Π group results which is merely the Reynolds number. The analysis below excludes density, however, the final example considers this problem with density as an additional variable.

Once again we examine the dimensional matrix and determine the order of the largest square sub-matrix which has a non-zero determinant.

	$-\frac{dp}{dz}$	$\overline{w}$	A	P	μ
M	1	0	0	0	1
L	-2	1	2	1	-1
T	-2	-1	0	0	-1

In this case the rank of the matrix is determined to be three. One set of repeating variables may be chosen to be $\overline{w}$, μ and A. Now Eq. (24) may be rewritten as

$$\phi(\pi_1, \pi_2) = 0 \tag{25}$$

Proceeding with the analysis results in the following Π groups:

$$\pi_1 = \frac{-\frac{dp}{dz} A}{\overline{w}\mu}, \quad \pi_2 = \frac{P}{\sqrt{A}} \tag{26}$$

Now in this case, since there are only two Π groups, Eq. (25) may be written in the following form:

$$\frac{-\frac{dp}{dz} A}{\overline{w}\mu} = C \frac{P}{\sqrt{A}} \tag{27}$$

or it may be expressed as

$$\frac{-\frac{dp}{dz} A}{\overline{w}\mu} \frac{\sqrt{A}}{P} = C \tag{28}$$

Finally, by performing a control volume force balance at the wall of the duct one arrives at the following relation:

$$-\frac{dp}{dz} A = \overline{\tau}_w P \tag{29}$$

This leads to the final form of the dimensionless wall shear stress

$$\frac{\overline{\tau}_w \sqrt{A}}{\overline{w}\mu} = C \tag{30}$$

This dimensionless group is sometimes referred to as the *Poiseuille* number Po[1,4]. In this case the characteristic length is the square root of the cross-sectional flow area $\mathcal{L} = \sqrt{A}$.

Finally, the hydrodynamic problem will be re-analyzed using the Π theorem while considering the fluid density as an additional variable. Therefore,

$$f(\overline{w}, -\frac{dp}{dz}, \mu, \rho, A, P) = 0 \tag{31}$$

The dimensional matrix for the new problem is

	$-\frac{dp}{dz}$	$\overline{w}$	A	P	μ	ρ
M	1	0	0	0	1	1
L	-2	1	2	1	-1	-3
T	-2	-1	0	0	-1	0

Analysis of the matrix above reveals that the rank is again three. The repeating variables may be chosen to be $\overline{w}$, ρ and A. This allows Eq. (31) to be written as

$$\phi(\pi_1, \pi_2, \pi_3) = 0 \tag{32}$$

Proceeding with the Π theorem analysis the following Π groups will be formed:

$$\pi_1 = \frac{-\frac{dp}{dz}\sqrt{A}}{\rho \overline{w}^2}, \quad \pi_2 = \frac{\mu}{\rho \overline{w} \sqrt{A}}, \quad \pi_3 = \frac{P}{\sqrt{A}} \tag{33}$$

The reader should recognize the first Π group as the definition of the Darcy friction factor with the characteristic length $\sqrt{A}$ in place of the hydraulic diameter D_h, and the second Π group as the reciprocal of the Reynolds number based upon $\mathcal{L} = \sqrt{A}$ in place of the hydraulic diameter D_h.

Equation (32) may be written in the more familiar form

$$\frac{-\frac{dp}{dz}\sqrt{A}}{\rho \overline{w}^2} = F\left(\frac{\mu}{\rho \overline{w} \sqrt{A}}, \frac{P}{\sqrt{A}}\right) \tag{34}$$

In all three applications of the Π theorem, the Π group $P/\sqrt{A}$ appeared. This dimensionless parameter appears to be an important geometric parameter which leads to the collapsing of the numerical data for many geometries onto a single curve. Finally, dimensional analysis also suggests that the characteristic length $\mathcal{L} = \sqrt{A}$ should be

used to non-dimensionalize the thermal and hydrodynamic problems, rather than the hydraulic or equivalent diameter $D_h = 4A/P$.

EFFECT OF LENGTH SCALES ON NON-DIMENSIONAL GROUPS

In the previous sections dimensional analysis predicted that the characteristic length for non-dimensionalizing the thermal and hydrodynamic problems should be $\mathcal{L} = \sqrt{A}$. The analysis also produced the geometric group $P/\sqrt{A}$. This parameter may be viewed as a geometric scaling factor such that

$$fRe_{\sqrt{A}} = fRe_{D_h}\left(\frac{P}{4\sqrt{A}}\right) \tag{35}$$

The additional factor of 4 arises from the definition of the hydraulic diameter. The solutions for several singly and doubly-connected domains will be re-analyzed using the results predicted by the dimensional analysis of the previous section. All of the results are presented in terms of the dimensionless group fRe since many solutions are available in the fluid mechanics literature[1,2,3]. The hydrodynamic and thermal prolems are related through Eq. (15) presented earlier.

Singly-Connected Domains

The fRe results for polygonal shapes are presented in Table 1 for the characteristic lengths $\mathcal{L} = 4A/P$ and $\mathcal{L} = \sqrt{A}$. Also presented in Table 1 is the ratio of the fRe result of the polygon to the fRe result of the circle for each case. It is clear from the fourth column of Table 1, that when $\mathcal{L} = \sqrt{A}$ is used, there is very little difference between the regular polygons and the circular geometry. The largest difference occurs with the triangular geometry. When $N \geq 4$, the difference is negligible. If the triangular geometry is excluded, the difference between the solutions for the polygonal domains and the circular domain is less than 0.2 percent.

Table 1
fRe Results for Polygonal Geometries[13,14]

N	fRe_{D_h}	$\left(\frac{fRe^P}{fRe^C}\right)_{D_h}$	$fRe_{\sqrt{A}}$	$\left(\frac{fRe^P}{fRe^C}\right)_{\sqrt{A}}$
3	13.33	0.833	15.19	1.071
4	14.23	0.889	14.23	1.004
5	14.73	0.921	14.04	0.990
6	15.05	0.941	14.01	0.988
7	15.31	0.957	14.05	0.991
8	15.41	0.963	14.03	0.989
9	15.52	0.970	14.04	0.990
10	15.60	0.975	14.06	0.992
20	15.88	0.993	14.13	0.996
∞	16	1.000	14.18	1.000

Figure 4 presents the results for the rectangular and elliptical geometries. The fRe results for these two geometries vary substantially with the aspect ratio b/a which is a ratio of the minor and major axes when $\mathcal{L} = 4A/P$.

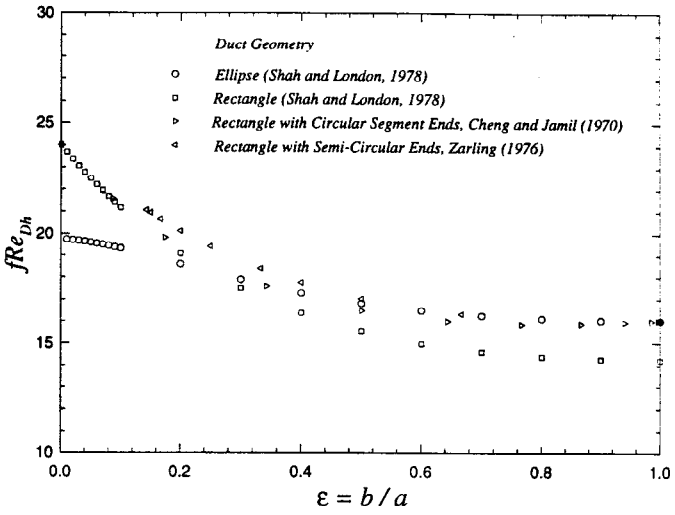

Fig. 4 fRe_{D_h} for singly-connected geometries

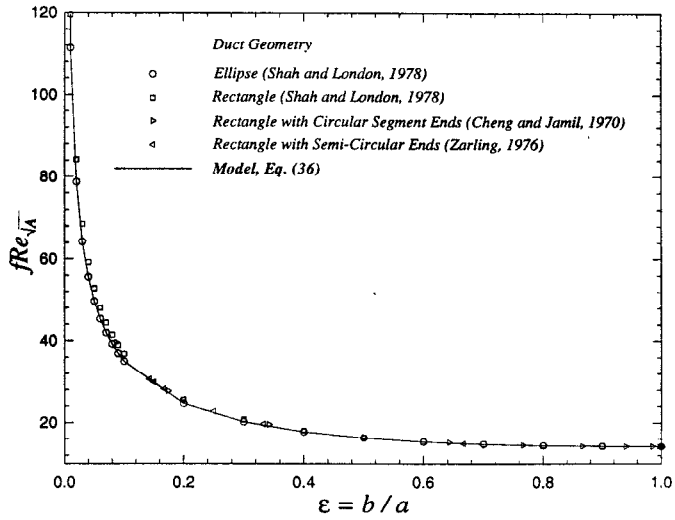

Fig. 5 $fRe_{\sqrt{A}}$ for singly-connected geometries

If the results are replotted according to Eq. (35), very little difference is observed between these geometries. Numerical values for the elliptic and rectangular geometries are presented in Table 2 for both definitions of $\mathcal{L}$. Also presented in Table 2 are the ratios of fRe results for the rectangular geometry and fRe results for the elliptic geometry at the corresponding aspect ratio. It may be seen from the last column of Table 2, that $\mathcal{L} = \sqrt{A}$ appears to be more appropriate than $\mathcal{L} = 4A/P$.

All of the results in Fig. 5 may be approximated by the solution for the elliptical geometry. The elliptical geometry was chosen to model all of the results since it has a closed form solution, whereas the rectangular geometry requires a series solution to describe the velocity or temperature distribution.

Table 2
fRe Results for Elliptical and Rectangular Geometries[3]

	fRe_{D_h}			$fRe_{\sqrt{A}}$		
b/a	Rectangular	Elliptical	$\left(\frac{fRe^R}{fRe^E}\right)_{D_h}$	Rectangular	Elliptical	$\left(\frac{fRe^R}{fRe^E}\right)_{\sqrt{A}}$
0.01	23.67	19.73	1.200	119.56	111.35	1.074
0.05	22.48	19.60	1.147	52.77	49.69	1.062
0.10	21.17	19.31	1.096	36.82	35.01	1.052
0.20	19.07	18.60	1.025	25.59	24.65	1.038
0.30	17.51	17.90	0.978	20.78	20.21	1.028
0.40	16.37	17.29	0.947	18.12	17.75	1.021
0.50	15.55	16.82	0.924	16.49	16.26	1.014
0.60	14.98	16.48	0.909	15.47	15.32	1.010
0.70	14.61	16.24	0.900	14.84	14.74	1.007
0.80	14.38	16.10	0.893	14.47	14.40	1.005
0.90	14.26	16.02	0.890	14.28	14.23	1.004
1.00	14.23	16.00	0.889	14.23	14.18	1.004

The general expression is

$$fRe_{\sqrt{A}} = 8\sqrt{\pi}\left(\frac{\pi}{4}\frac{(1+\epsilon^2)}{\sqrt{\epsilon}\,E(\sqrt{1-\epsilon^2})}\right) \tag{36}$$

where $E(\cdot)$ is the complete elliptic integral of the second kind and $0 \leq \epsilon = \frac{b}{a} \leq 1$ is the aspect ratio of the geometry. To eliminate the problem of evaluating the elliptic integral, an approximate expression was developed for the shape function $g(\epsilon)$ defined as

$$g(\epsilon) = \left(\frac{\pi}{4}\frac{1+\epsilon^2}{\sqrt{\epsilon}E(\sqrt{1-\epsilon^2})}\right) \tag{37}$$

such that

$$fRe_{\sqrt{A}} = 8\sqrt{\pi}g(\epsilon) \tag{38}$$

The shape function $g(\epsilon)$ may be accurately computed from the following expression:

$$g(\epsilon) \approx \left[(1/0.92)^{1-\epsilon}(\sqrt{\epsilon} - \epsilon^{3/2}) + \epsilon\right]^{-1} \tag{39}$$

Equation (39) is valid over the range $0.05 \leq \epsilon \leq 1$ with an RMS error of 0.70 percent and a maximum error less than ± 2 percent.

Doubly-Connected Domains

Another useful group of geometries are the polygonal annular geometries. Several variations are possible. They may be circular-polygonal, polygonal-circular, or a combination of similar polygons which are concentric. Only the first two of these cases were examined in the literature by Ratkowsky and Epstein[15] and Hagan and Ratkowsky[16]. The results are plotted in Fig. 6 for the case of a circular boundary with a polygonal core and a polygonal boundary with circular core. At first sight, these appear to be very different geometries. However, if the fRe results are based upon the square root of the flow area, $\sqrt{A_o - A_i}$, and a more suitable aspect ratio defined as $\beta = \sqrt{A_i/A_o}$, the results are identical to the results predicted by the solution for the circular annular geometry for a wide range of β as shown in Fig. 7. The solution for the circular annular geometry is given by

$$fRe_{\sqrt{A}} = 8\sqrt{\pi}\left[\frac{(1-\beta)\sqrt{1-\beta^2}}{1+\beta^2-\frac{1-\beta^2}{\ln(1/\beta)}}\right] \tag{40}$$

where $\beta = \sqrt{A_i/A_o}$, which reduces to $\beta = r_i/r_o = r^*$ for the circular annulus.

As the inner boundary approaches the outer boundary several smaller regions are formed. At this point the domain is no longer doubly-connected, but is now composed of several singly-connected areas in parallel. Thus the definitions of flow area and aspect ratio are no longer valid in this region. The area should now be based upon the area of the singly-connected domain and the aspect ratio defined in terms of this new geometry. It is for these reasons that the results diverge from the solution of the circular annular region in Fig. 7. The $fRe_{\sqrt{A}}$ results may be predicted from the expression for the singly-connected regions, with the appropriate aspect ratio ϵ.

For most practical applications the value of β is such that the numeric values of the $fRe_{\sqrt{A}}$ may be accurately computed from the solution for the circular annulus. Table 3 summarizes the critical and maximum values of

$\beta = \sqrt{A_i/A_o}$ for the data of Ratkowsky and Epstein[15] and Hagan and Ratkowsky[16].

Finally, it may be reasonable to expect the results for concentric homologous polygons, i.e. triangle-triangle, square-square, (see Fig. 3), to behave approximately as a concentric circular annulus for the entire range of $\beta = \sqrt{A_i/A_o}$.

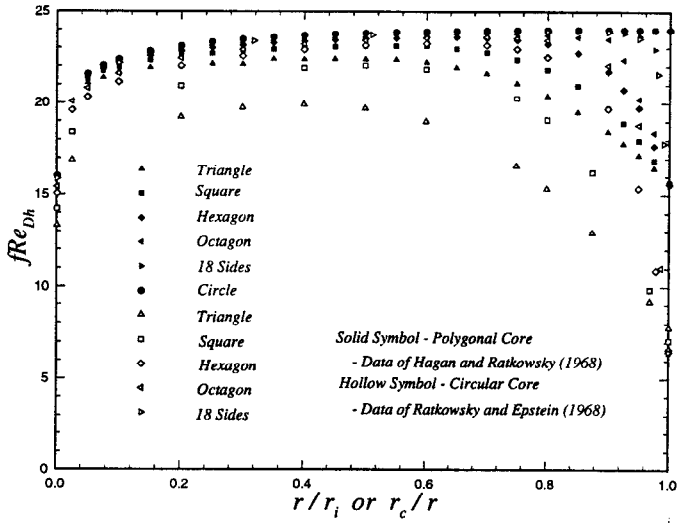

Fig. 6 fRe_{D_h} for doubly-connected geometries

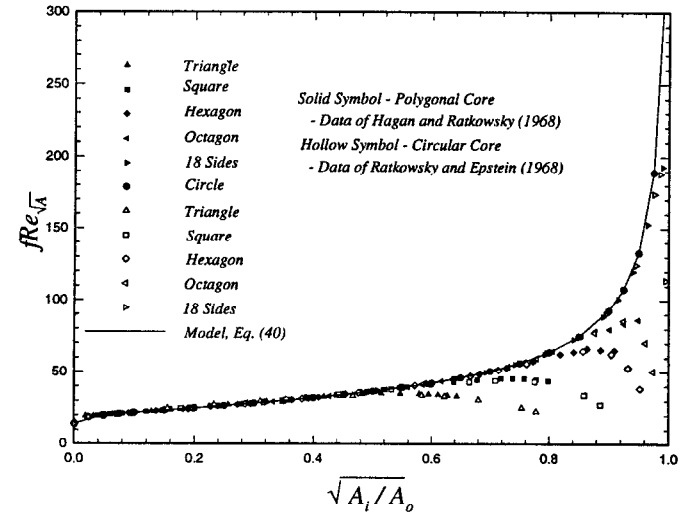

Fig. 7 $fRe_{\sqrt{A}}$ for doubly-connected geometries

Other Singly-Connected Domains

A comparison of the proposed model for other singly-connected domains is presented below in Figs. 8-11 and in Table 4. The fRe results are shown for both $\mathcal{L} = 4A/P$ and $\mathcal{L} = \sqrt{A}$. The additional geometries of interest are the isosceles triangle[17], right triangle[18], circular sector[19], circular segment[20], sinusoid[17], rhombus[17], cusp shapes[13,15,21] and the circular annular sector[3]. The results for two other geometries, namely the circular duct with diametrically opposed flat sides[22], and the rectangular duct with semi-circular ends[23], are presented in Figs. 4 and 5 along with the elliptic and rectangular geometries. All of the results are plotted versus an aspect ratio ϵ. The aspect ratio ϵ is defined as the ratio of the maximum width and height of each geometry with the constraint that $0 < \epsilon < 1$.

Table 3
Critical and Maximum Values of $\sqrt{A_i/A_o}$

N	Critical Values	Maximum Values	
		Polygonal Core	Circular Core
3	0.52	0.643	0.778
4	0.68	0.798	0.886
6	0.80	0.910	0.952
8	0.88	0.949	0.974
18	0.96	0.990	0.995
∞	1.000	1.000	1.000

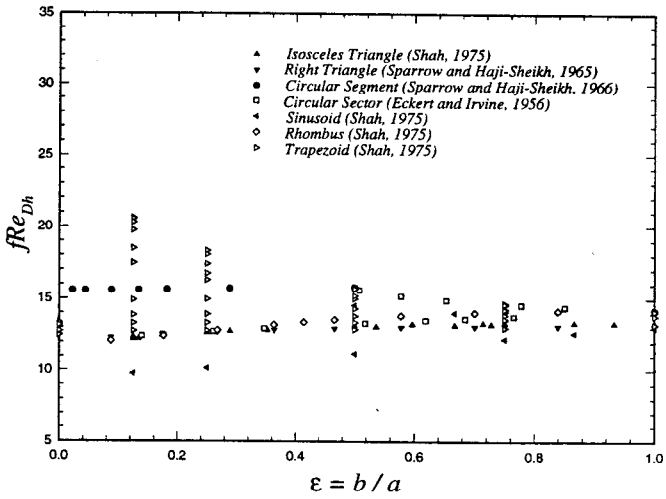

Fig. 8 fRe_{D_h} for singly-connected geometries

The numerical results for these geometries do not display any clear trend versus the aspect ratio ϵ in Fig. 8. Some geometries show an increase in fRe_{D_h} with decreasing ϵ, while others decrease with decreasing ϵ. When the results are presented in terms of $fRe_{\sqrt{A}}$ as shown in Fig. 9 the trend is quite clear, all geometries have $fRe_{\sqrt{A}}$ which increase with a decrease in ϵ. The results for these other geometries are predicted reasonably well by Eq. (36) for $\epsilon > 0.4$. At lower values of ϵ, the effect of small corner angles is quite prominent. However, most of the results are predicted by Eq. (36) within ± 10 percent as shown in Fig. 9.

The results for the circular annular sector are presented in Figs. 10 and 11. For this geometry the aspect ratio is defined as the ratio of the spacing of the annular sector $(r_o - r_i)$ to the average arc length $(r_o + r_i)\Phi$ such that $0 < \epsilon < 1$. As the value of $r^* = r_i/r_o \to 0$, the annular sector becomes a circular sector and the definition of the aspect ratio is no longer appropriate. However, as

the value of $r^* = r_i/r_o \to 1$ the annular sector becomes a curved rectangular geometry and the definition is compatible with that of the rectangular geometry. For comparative purposes, the results for the circular sector are plotted along with the results for the annular sector in Fig. 11.

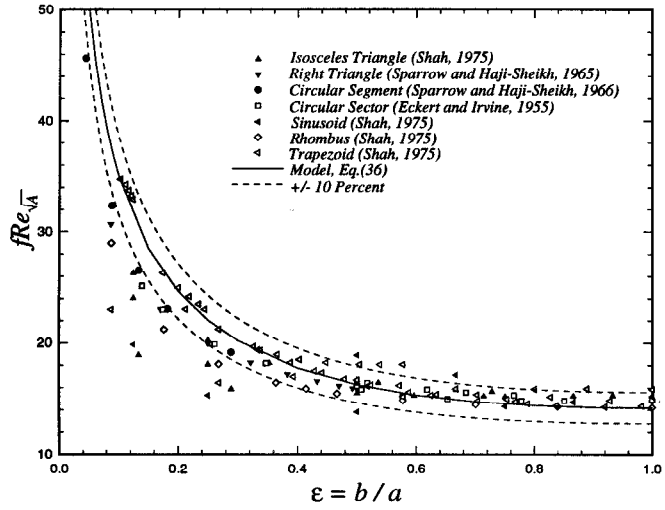

Fig. 9 $fRe_{\sqrt{A}}$ for singly-connected geometries

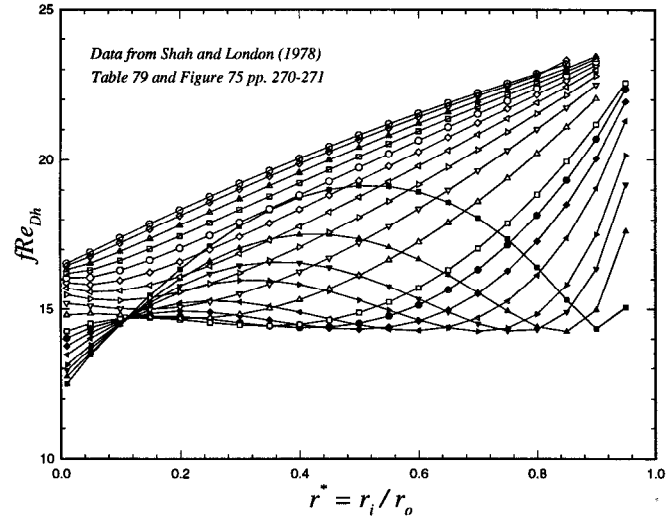

Fig. 10 fRe_{D_h} for circular annular sector

This comparison illustrates the importance of the definition of aspect ratio. At small values of ϵ which correspond to small values of r^*, the definition of the aspect ratio needs to be modified to the ratio of the radius and chord length of the sector as shown in Fig. 2. It is for this reason that a few of the data points in Fig. 11 are not predicted by the model defined by Eq. (36).

Finally, for the cusp shaped geometries shown in Fig. 2, the results are approximately equal to the value for the circular duct provided that the characteristic length is taken to be $\mathcal{L} = \sqrt{A}$. The results for these geometries are presented in Table 4. Application of this analysis demonstrates that $\mathcal{L} = \sqrt{A}$ appears to be more appropriate than $\mathcal{L} = 4A/P$, for both the thermal and hydrodynamic problems.

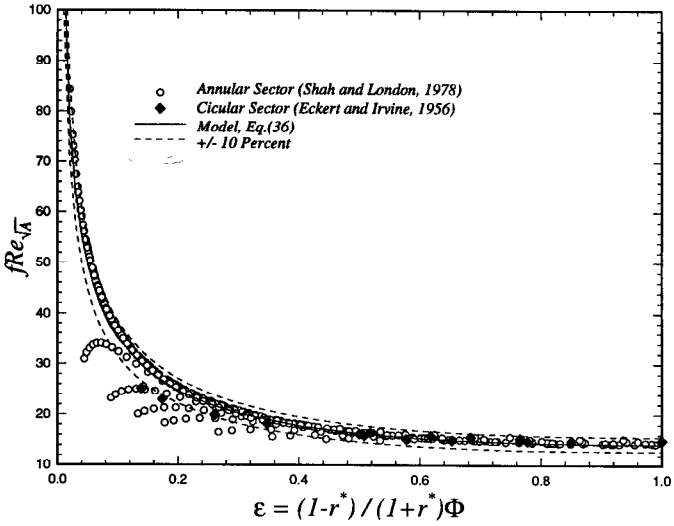

Fig. 11 $fRe_{\sqrt{A}}$ for circular annular sector

Table 4
fRe for Various Cusps[13,15,21]

Geometry	fRe_{D_h}	$fRe_{\sqrt{A}}$
Square Corner Cusp	7.06	13.60
Triangular Corner Cusp	7.80	13.10
Side Cusp	6.50	12.75
3 Sided Cusp	6.50	12.72
4 Sided Cusp	6.61	11.20
Circular Duct	16.00	14.18

SUMMARY AND CONCLUSIONS

This paper examined solutions to Poisson's equation in singly and doubly-connected domains with applications in heat conduction and fluid mechanics. By means of dimensional analysis using the Buckingham Π theorem, the appropriate non-dimensional form and characteristic length were obtained. Simple expressions for predicting the non-dimensional groups were developed for the singly and doubly-connected domains. These solutions represent the exact solutions for the elliptic geometry and circular annular geometry. The characteristic length based upon the square root of the effective cross-sectional area $\mathcal{L} = \sqrt{A}$ was found to be more useful in collapsing the results of similar geometries than the characteristic length $\mathcal{L} = 4A/P$, also known as the hydraulic diameter. It was shown that if the characteristic length $\mathcal{L} = \sqrt{A}$ is used to non-dimensionalize the solutions, the dimensionless groups are weak functions of the shape of the geometry, provided the an appropriate aspect ratio is defined. Definitions of aspect ratio for various geometries are summarized below in Table 5. The results for 27 singly-connected domains and 9 doubly-connected domains are accurately predicted by the solutions for the elliptic geometry Eq. (36) and circular annulus Eq. (40) respectively, when the appropriate aspect

ratio is defined. Finally, the relation between the thermal and hydrodynamic problem was examined such that solutions[3,24] for other complex geometries not examined in this paper may be applied to thermal problem.

Table 5
Definitions of Aspect Ratio

Geometry	Aspect Ratio
Regular Polygons	$\epsilon = 1$
Singly-Connected‡	$\epsilon = \frac{b}{a}$
Trapezoid	$\epsilon = \frac{2b}{a+c}$
Annular Sector	$\epsilon = \frac{1-r^*}{(1+r^*)\Phi}$
Doubly-Connected	$\beta = \sqrt{\frac{A_i}{A_o}}$

‡ All except annular sector and trapezoid.

ACKNOWLEDGEMENTS

The authors acknowledge the financial support of the Natural Sciences and Engineering Research Council operating grant A7455, the Manufacturing Research Corporation of Ontario and Long Manufacturing of Oakville, Ontario. The authors also acknowledge the assistance of Mirko Stevanović and Peter Teertstra in the preparation of the figures.

REFERENCES

[1]White, F.M., *Viscous Fluid Flow*, McGraw-Hill, New York, NY, 1991.

[2]Happel, J. and Brenner, H., *Low Reynolds Number Hydrodynamics*, Noordhoff International Publishing, 1965.

[3]Shah, R.K. and London, A.L., *Laminar Forced Flow Convection in Ducts*, Academic Press, New York, NY, 1978.

[4]Churchill, S.W., *Viscous Flows: The Practical Use of Theory*, Butterworths, Boston, MA, 1988.

[5]Huntly, E.S., *Dimensional Analysis*, Rinehart, New York, NY, 1951.

[6]Langhaar, H.L., *Dimensional Analysis and Theory of Models*, Wiley, New York, NY, 1951.

[7]Taylor, E.S., *Dimensional Analysis for Engineers*, Oxford University Press, Oxford, 1974.

[8]Vennard, J.L. and Street, R.L., *Elementary Fluid Mechanics*, Wiley, New York, NY, 1982.

[9]White, F.M., *Fluid Mechanics*, McGraw-Hill, New York, NY, 1987.

[10]McAdams, W.H., *Heat Transmission*, McGraw-Hill, New York, NY, 1942.

[11]Rohsenow, W.M. and Choi, H.Y., *Heat, Mass, and Momentum Transfer*, Prentice-Hall, Englewood Cliffs, NJ, 1961.

[12]Panton, R.L., *Incompressible Flow*, Wiley, New York, NY, 1985.

[13]Shih, F.S., "Laminar Flow in Axisymmetric Conduits by a Rational Approach", *Canadian Journal of Chemical Engineering*, Vol. 45, 1967, pp. 285-294.

[14]Cheng, K.C., "Laminar Flow and Heat Transfer Characteristics in Regular Polygonal Ducts", *Proceedings of the International Heat Transfer Conference, 3rd AIChE*, Vol. 1, 1966, pp. 64-76.

[15]Ratkowsky, D.A. and Epstein, N., "Laminar Flow in Regular Polygonal Shaped Ducts with Circular Centered Cores", *Canadian Journal of Chemical Engineering*, Vol. 46, 1968, pp. 22-26.

[16]Hagan, S.L. and Ratkowsky, D.A., "Laminar Flow in Cylindrical Ducts Having Regular Polygonal Shaped Cores", *Canadian Journal of Chemical Engineering*, Vol. 46, 1968, pp. 387-388.

[17]Shah, R.K., "Laminar Flow Friction and Forced Convection Heat Transfer in Ducts of Arbitrary Geometry", *International Journal of Heat and Mass Transfer*, Vol. 18, 1975, pp. 849-862.

[18]Sparrow, E.M. and Haji-Sheikh, A., "Laminar Heat Transfer and Pressure Drop in Isoceles Triangular, Right Triangular, and Circular Sector Ducts", *Journal of Heat Transfer*, Vol. 87, 1965, pp. 426-427.

[19]Eckert, E.R.G. and Irvine, T.F., "Flow in Corners of Passages with Non-Circular Cross-sections", *Transactions of the ASME*, Vol. 78, 1956, pp. 709-718.

[20]Sparrow, E.M. and Haji-Sheikh, A., "Flow and Heat Transfer in Ducts of Arbitrary Shape with Thermal Boundary Conditions", *Journal of Heat Transfer*, Vol. 91, 1966, pp. 351-358.

[21]Gunn, D.J. and Darling, C.W.W., "Fluid Flow and Energy Losses in Non-Circular Conduits", *Transactions of the Institution of Chemical Engineers*, Vol. 41, 1963, pp. 163-173.

[22]Cheng, K.C. and Jamil, M., "Laminar Flow and Heat Transfer in Circular Ducts with Diametrically Opposite Flat Sides and Ducts of Multiply Connected Cross Sections", *Canadian Journal of Chemical Engineering*, Vol. 48, 1970, pp. 333-334.

[23]Zarling, J.P., "Application of Schwarz-Neumann Technique to Fully Developed Laminar Heat Transfer in Non-Circular Ducts", *Journal of Heat Transfer*, Vol. 99, 1976, pp. 332-335.

[24]Shah, R.K. and Bhatti, M.S., *Chapter 3: Laminar Convective Heat Transfer in Ducts*, in *Handbook of Single Phase Convective Heat Transfer*, eds. S. Kakac, R.K. Shah and W. Aung, John Wiley and Sons Inc., 1987.